Photonics-Based Microwave Switching Using Optical Single Sideband Wavelength Conversion in a Semiconductor Optical Amplifier

Dan Zhu, *Member, IEEE*, Zhengwu Wei, Huan Wu, and Shilong Pan, *Senior Member, IEEE*

***Abstract*— Photonics-based microwave switching using optical single sideband (OSSB) wavelength conversion in a semiconductor optical amplifier (SOA) is proposed and demonstrated. By using the joint four-wave mixing and self-phase modulation effects in the SOA, the scheme can simultaneously realize the OSSB signal generation and photonic microwave switching, which can minimize the switching crosstalk, since the OSSB signal occupies the least optical bandwidth. This method is also simple as only a single SOA is required. Photonic switching of a 200-Mb/s 16-QAM signal centered at 20 GHz is performed. The signal after switching is an OSSB signal, which has a 22.65- or 17.85-dB sideband suppression ratio for switching based on wavelength down- or up-conversion, respectively. An investigation with the switched signals to combat the dispersion-induced power fading effect for radio over fiber application is also taken. Performance dependence of the optical pump and probe powers, the optical probe-pump power ratio, the modulation depth of the probe signal, and the SOA bias current are also investigated and analyzed.**

***Index Terms*— Microwave photonics, optical single sideband (OSSB), photonic microwave switching, radio over fiber (RoF), semiconductor optical amplifier (SOA).**

I. Introduction

RADIO over fiber (RoF) has been considered a promising way for broadband wireless communication, antenna remoting, and radar applications [1]–[4]. To realize system reconfiguration, function switching, or signal routing of RoF systems, RF switching is always required [1]–[6]. As compared with pure electronic switching technologies, the limitations with electromagnetic isolation, working bandwidth, and switching speed can be broken through by photonic microwave switching due to the photonic technologies' advantages. Previously, optical RF switching was realized using the semiconductor optical amplifiers (SOAs), because the ON- and OFF-states of the SOAs can be achieved by simply controlling their bias currents [1], [7], [8]. A very high switching speed can be achieved due to the nanosecond-level rise or fall time supported by the SOAs. In addition, an SOA itself can provide optical gain and is capable to be integrated with other optical components. However, a switching matrix consisting of a large number of SOAs is always needed, so the system is complicated and costly.

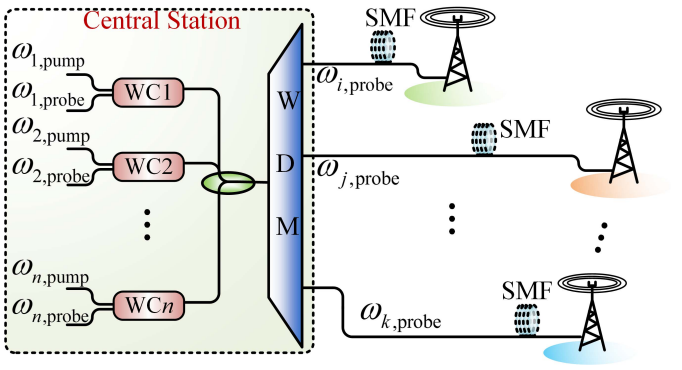

Fig. 1. Photonic microwave switching for RoF systems based on wavelength conversion. WC: wavelength converter. SMF: single-mode fiber. WDM: wavelength division demultiplexer.

Wavelength conversion via nonlinear effects in the SOAs can also be used to realize photonic microwave switching, such as cross-phase modulation (XPM) effect, cross-gain modulation (XGM) effect, or four-wave mixing (FWM) effect [9]–[11]. Fig. 1 shows the typical scheme of an $N \times N$ photonic microwave switch based on wavelength conversion. Different wavelength channels correspond to different output ports. To avoid crosstalk between these outputs, which would be a serious problem in analog systems, every signal after wavelength conversion should be restricted in one wavelength channel. However, the conventional microwave modulated optical signal after wavelength conversion [9]–[11] is a double-sideband (DSB) modulated signal, i.e., both the upper and lower sides of the optical carrier are modulated with the same RF signal, which occupies a wide optical bandwidth, making the sidebands easily leaking to the neighboring outputs. To minimize the possibility of leakage, in this paper, we will propose to generate optical single sideband (OSSB) modulated signal within the wavelength converter. Apart from the least optical bandwidth, OSSB modulation can also overcome the dispersion-induced RF power fading problem, especially for long-distance RoF applications [12].

In general, OSSB modulation can be achieved by using optical filters to remove the unwanted optical sidebands

Manuscript received November 16, 2015; revised February 2, 2016, August 7, 2016, and September 20, 2016; accepted September 23, 2016. Date of publication October 13, 2016; date of current version January 26, 2017. This work was supported in part by the National Natural Science Foundation of China under Grant 61527820 and Grant 61422108, and in part by the Natural Science Foundation of Jiangsu Province under Grant BK20160082.

The authors are with the Key Laboratory of Radar Imaging and Microwave Photonics, Ministry of Education, Nanjing University of Aeronautics and Astronautics, Nanjing 210016, China (e-mail: pans@ieee.org).

Color versions of one or more of the figures in this paper are available online at http://ieeexplore.ieee.org.

Digital Object Identifier 10.1109/TMTT.2016.2614293

of a DSB-modulated signal [13], optical injection locking of laser diodes [14], using stimulated Brillouin scattering effect [15], or by incorporating a dual-drive Mach–Zehnder modulator (MZM) together with a 90° or 120° electrical hybrid [12], [16], [17]. The nonlinear effects in the SOAs can also be used to implement OSSB [18]–[21]. In [18], self-phase modulation (SPM) in an SOA, which introduces a $\pi/2$-phase difference to the phase and amplitude terms of a DSB modulated optical signal, is employed to realize the OSSB modulation. The sideband suppression ratio (SSR) can be further improved by using the polarization dependence of the SPM and self-gain modulation effects [19]. However, the polarization-dependent operation would make the system sensible to environmental variation. Quasi-OSSB modulation can also be realized based on the coherent population oscillation effects in a nonlinear SOA [20], but the SSR is usually small. In [21], an SOA-based OSSB modulation is realized by using the XPM and FWM effects. However, both the probe and pump lights should be modulated, and the modulated probe and pump signals' phase difference must be adjusted precisely. In addition, for the previously reported schemes, the photonic microwave switching and the OSSB modulation are usually achieved by using two different schemes, which makes the system bulky and complicated. Thus, realizing the two functions simultaneously in the same scheme is highly desirable to make the system simple and suitable for RoF applications.

Recently, we have proposed a novel approach to implement the photonic microwave switching using OSSB wavelength conversion in an SOA [22]. The photonic microwave switching and OSSB modulation are simultaneously realized in a single scheme. Due to the use of FWM effect, the switching system also has the special feature of being transparent with modulation format and data rate for a large wavelength working range. This feature is very important, since the RoF applications are usually required to handle large-bandwidth analog signals. However, it is insufficient to understand the approach, since only some preliminary experimental results are reported.

In this paper, a comprehensive theoretical and experimental investigation is performed on the photonic microwave switching based on OSSB wavelength conversion. Section II introduces the principle of the proposed photonics-based microwave switching using OSSB wavelength conversion in an SOA. In Section III-A, photonic microwave switching of a 200-Mb/s 16-QAM signal centered at 20 GHz is performed experimentally, and a simultaneous OSSB modulation of the switched signal with 22.65- and 17.85-dB SSR is realized for wavelength down- and up-conversion, respectively. An investigation of the transmission performance of the OSSB switched signals in an optical link is also taken in Section III-A. Section III-B investigates the influence of the key parameters of pump and probe powers, the modulation depth of the probe signal and the SOA bias current. Section IV gives the conclusion.

II. Principle

The simplified configuration of the proposed photonic microwave switching (i.e., $1 \times N$ scheme) is shown in Fig. 2.

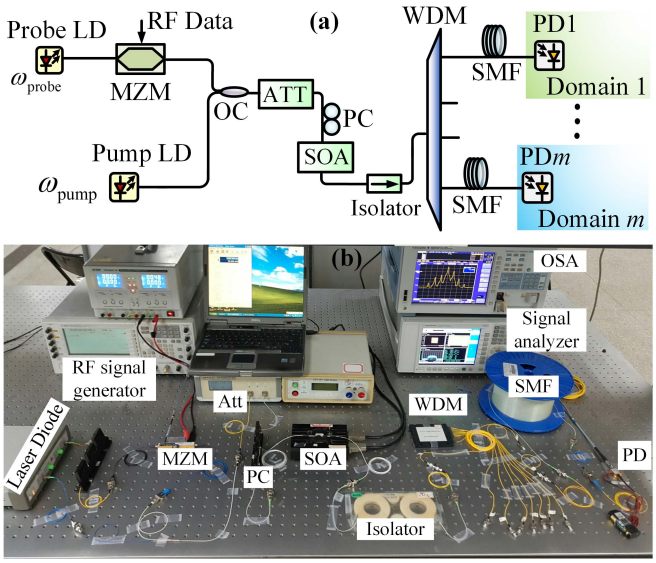

Fig. 2. (a) Configuration and (b) experimental setup of the proposed OSSB wavelength conversion-based photonic microwave switch. PC: polarization controller. ATT: attenuator. MZM: Mach–Zehnder modulator. SMF: single-mode fiber. OC: optical coupler. SOA: semiconductor optical amplifier. WDM: wavelength division demultiplexer. PD: photodetector.

An RF signal of Ω_m is modulated on a lightwave with a frequency of ω_{probe} at an MZM to generate a DSB-modulated probe signal. A continuous wave pump of ω_{pump} is then coupled with the probe signal and injected into an SOA. The injected optical power is controlled by a tunable optical attenuator. The SOA used in the scheme is assumed to be polarization-independent, so the FWM's polarization dependence is not considered [23]. The FWM effect in the SOA generates two new components at $\omega_{\text{cs}} = 2\omega_{\text{pump}} - \omega_{\text{probe}}$ and $\omega_{\text{idle}} = 2\omega_{\text{probe}} - \omega_{\text{pump}}$, respectively [24]. By using an optical filter, the signal at ω_{cs} can be selected. Denoting the optical field of the optical pump and probe signal as E_{pump} and E_{probe}, respectively, the signal generated at ω_{cs} can be written as [8], [25]

$$E_{\text{cs}} = -\frac{1}{2}\left[\frac{1-i\alpha}{1-i\omega_{\text{d}}\tau_c}\cdot\frac{1}{I_s} + \frac{1-i\beta}{1-i\omega_{\text{d}}\tau_n}\cdot\frac{1}{I_n}\right] \times |E_{\text{pump}}|^2 E^*_{\text{probe}} \tag{1}$$

where α is the SOA's linewidth enhancement factor, $\omega_d = \omega_{\text{pump}} - \omega_{\text{probe}}$ is the frequency detuning, τ_n and τ_c are the relaxation time constants for nonlinear gain and carrier density modulation, I_n and I_s are the saturation powers for nonlinear gain and carrier density modulation, and β denotes the real and imaginary parts ratio of the gain nonlinearity induced refractive index change. As can be seen, the generation of FWM signal consists of the contribution from the nonlinear gain and the carrier density modulation, and the signal at ω_{cs} is the replica of the optical probe with a conjugated phase.

Meanwhile, the optical probe experiences the SPM effect in the SOA, introducing a phase difference of ϕ between the frequency component in the amplitude ($\sim\sin(\Omega_m t)$) and that in the phase ($\sim\sin(\Omega_m t + \phi)$) [18], [19]. Taking into account

the SPM effect in the SOA, (1) can be rewritten as

$$E_{\mathrm{cs}} = -\frac{1}{2}\left[\frac{1-i\alpha}{1-i\omega_{\mathrm{d}}\tau_c}\cdot\frac{1}{I_s}+\frac{1-i\beta}{1-i\omega_{\mathrm{d}}\tau_n}\cdot\frac{1}{I_n}\right]|E_{\mathrm{pump}}|^2 \cdot E_0\left[1+\frac{m}{2}\sin(\Omega_m t)\right] \times \exp\left\{-i[\omega_{\mathrm{cs}}t+\frac{m\varepsilon}{2}\sin(\Omega_m t+\phi)]\right\} \quad (2)$$

where E_0 is the amplitude of the carrier, m is the RF modulation index, and ε denotes the chirp parameter of the SPM. According to [18], ϕ is close enough to $\pi/2$ at high frequency, so an OSSB modulation at the optical carrier of ω_{cs} is realized. In this way, the RF signal is transferred from the optical carrier of ω_{probe} to ω_{cs} by using the nonlinear effects of the SPM and FWM, and an OSSB modulation is simultaneously realized. By carefully selecting ω_{probe} or ω_{pump}, ω_{cs} can fall in the wavelength span of one channel of a wavelength division demultiplexer (WDM), so the RF signal carried by the OSSB signal with the optical carrier frequency of ω_{cs} is directed to a targeted path.

The proposed scheme could have a wide wavelength range, since the FWM effect is nearly free of phase mismatching problem [24], [26]. The wavelength range of the FWM-based wavelength conversion can be further increased if an SOA with longer active region is applied. For example, an SOA with 1.5-mm-long active region enabled wavelength down-conversion within a 30-nm range and up-conversion with a 15-nm range [27]. In addition, from (2), the SSR of the switched OSSB signal is determined by ϕ. When ϕ is exactly $\pi/2$, a switched OSSB signal with one sideband completely suppressed will be achieved, and when ϕ is deviated from $\pi/2$, the SSR will be decreased. According to [19], ϕ is given by

$$\phi = \pi - \arctan(\Omega_m \cdot \tau_{\mathrm{eff}}) \quad (3)$$

where τ_{eff} is the SOA's effective carrier recovery time. For a certain value of τ_{eff}, ϕ is close enough to $\pi/2$ if Ω_m is sufficiently large, and the larger Ω_m is, the larger the SSR will be. Therefore, the proposed scheme can allow a large RF bandwidth especially in the high-frequency regime.

III. Experimental Results and Analyses

An experiment is performed with the setup shown in Fig. 2. A tunable laser source with four channels (Agilent N7714A) is used to provide the probe and the pump lightwaves, and the wavelength stability is 2.5 pm. The MZM (Fujitsu FTM7938EZ-A) has a 40-GHz working bandwidth and a 2.1-V half-wave voltage. The bandwidth and responsivity of the PD (u^2t, XPDV21xxR) is 50 GHz and 0.65 A/W, respectively. The SOA (Kamelian SOA-NLL1-C-FA) has a 25-ps gain recovery time and a 1-dB polarization dependence. A PC is inserted before the SOA to adjust the polarization state. A vector signal generator (Agilent E8267D) is used to generate the RF signals. An eight-channel standard WDM with 200-GHz channel spacing is introduced to select the switched signal. The optical spectra are observed with an optical spectrum analyzer (Yokogawa AQ 6370C) with a 0.02-nm resolution, and a signal analyzer (Agilent N9030A) is used to measure the electrical signal before and after switching. In addition, the transmission performance of the switched OSSB signal is evaluated with a vector network analyzer (Agilent N5230A).

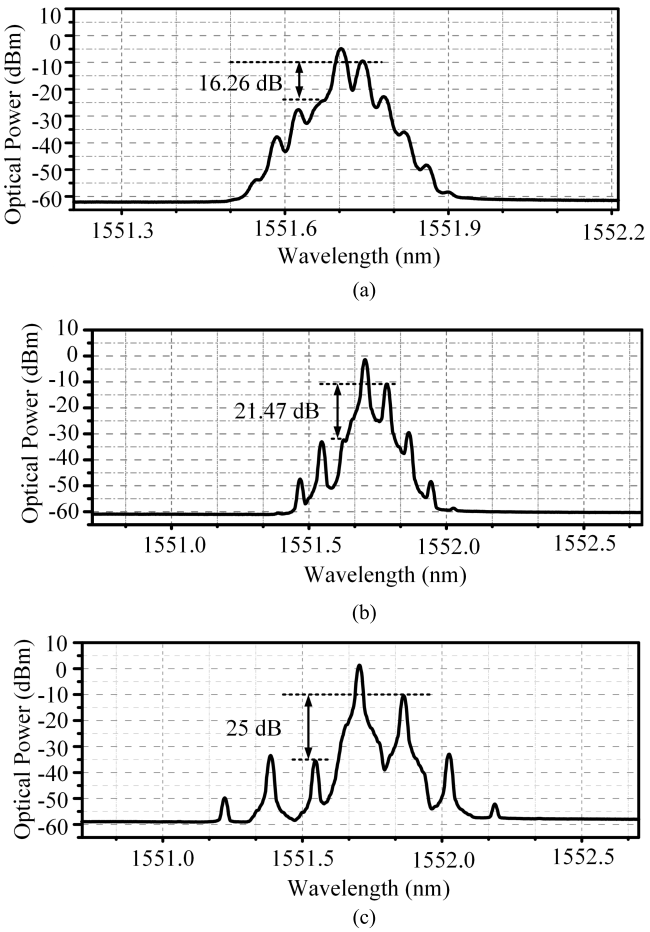

Fig. 3. Measured 1551.71-nm probe signal carrying an RF signal with a frequency of (a) 5, (b) 10, and (c) 20 GHz after the SOA when the pump is disconnected.

A. OSSB Wavelength-Based Photonic Microwave Switching

The OSSB wavelength conversion-based photonic microwave switching is verified. The wavelengths of the probe and the pump are fixed at 1551.71 and 1550.14 nm, respectively. When the optical carrier wavelength after conversion (ω_{cs}) is shorter than that before conversion (ω_{probe}), a wavelength down-conversion is performed. A 200-Mb/s 16-QAM signal with a power of 6 dBm is modulated on the probe lightwave. The power of the optical probe injected into the SOA is 2.41 dBm, and that of the optical pump is 2.52 dBm. Thus, the optical probe-pump ratio is calculated to be −0.11 dB. The SOA is biased at 185 mA.

First, OSSB generation based on the SPM effect in the SOA is investigated by only injecting the probe signal into the SOA and disconnecting the pump signal. In order to investigate the relationship between the SSR and the modulating RF frequency, RF signals with the frequencies of 5, 10, and 20 GHz are used. The measured optical spectra of the output signals are shown in Fig. 3. As can be seen, the OSSB signals are realized. The SSR, defined as the two first-order sidebands' power ratio,

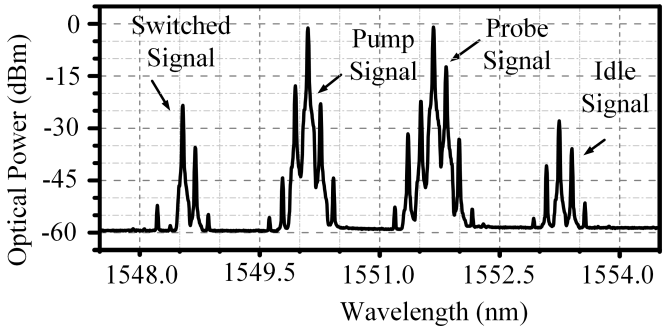

Fig. 4. Measured optical spectrum of the output signal with both the probe and pump signals injecting into the SOA.

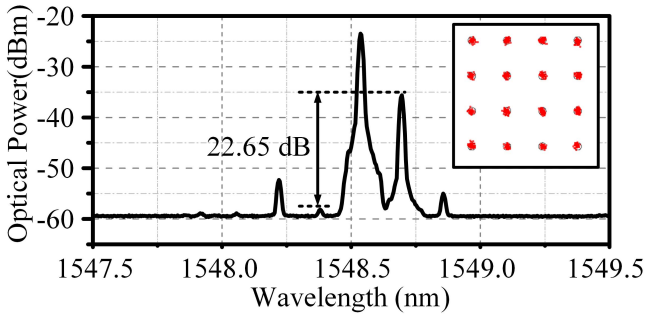

Fig. 5. Measured optical spectrum of the switched signal with the optical carrier wavelength of 1548.553 nm. Inset: measured constellation diagram of the switched signal with a −2-dBm received optical power injected into the PD.

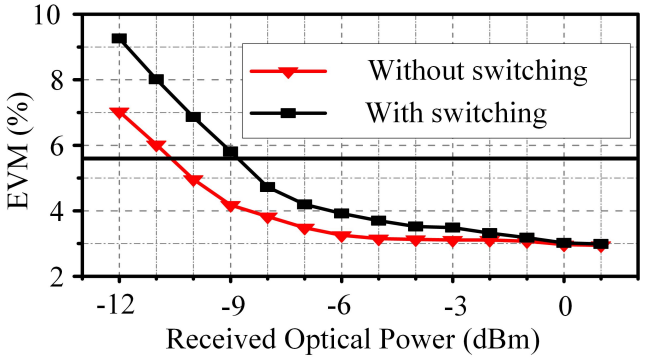

Fig. 6. Measured EVM values versus the optical power received by the PD without and with photonic microwave switching based on wavelength down-conversion.

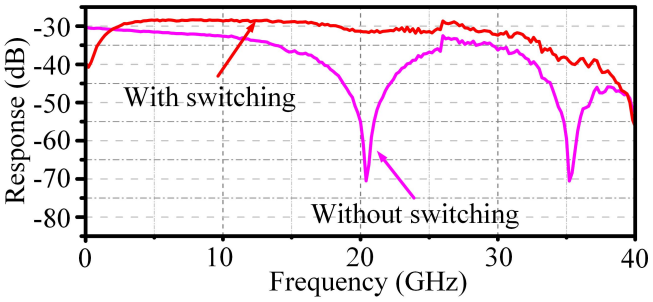

Fig. 7. Measured transmission responses over a 9-km optical link with and without the photonic microwave switching based on wavelength down-conversion.

is 16.26, 21.47, and 25 dB, respectively, which increases with the increasing of the modulated RF frequency. This phenomenon agrees well with the relationship between ϕ and Ω_m indicated in (3), showing that the phase and amplitude terms of the frequency component have a phase difference with the value of nearly $\pi/2$, which is indeed introduced by the SPM effect in the SOA [18], [19].

Then, with both the probe and pump signals being injected into the SOA, the joint FWM and SPM effects in the SOA will enable simultaneous wavelength conversion and OSSB generation. Fig. 4 shows the optical spectrum of the SOA's output when a 200-Mb/s 16-QAM signal centered at 20 GHz is modulated on the probe lightwave. As expected, the information carried by the probe is successfully copied to 1548.553 nm, and the wavelength-converted signal is an OSSB signal. If a WDM is followed, the information will be switched to the channel that covers 1548.553 nm. By adjusting the pump or probe wavelengths, different wavelength carrying the RF signal can be obtained, which will be directed to different channels by the WDM. Photonic microwave switching is thus implemented. The signal at the pump wavelength is also modulated, which is resulted by the XGM effect in the SOA.

Via the WDM, the switched signal with the carrier wavelength of 1548.33 nm will be selected and the other signals will be rejected. In this way, the overlapping of the idler signals to the wanted wavelength-converted signals will be avoided. Fig. 5 shows the switched signal with the optical carrier wavelength of 1548.33 nm. Accompanied with the wavelength conversion, OSSB modulation is implemented. The SSR is 22.65 dB, ∼3 dB smaller than the case with only the probe signal being injected into the SOA. It is because the pump signal's presence changes the carrier density in the SOA, leading to a different ϕ in (2). With −2 dBm received optical power injected into the PD, a 3.019% error vector magnitude (EVM) value is achieved with the switched signal. Fig. 5 (inset) shows the constellation diagram, confirming the good quality of the switched signal.

Fig. 6 shows the EVM values versus the optical power received by the PD without and with the proposed switching, where the condition without switching gives the back-to-back curve. By applying the 5.6% EVM threshold [28], the power penalty, which is the received optical power's increasing to get the same EVM value, is only 1.81 dB. The main contribution of the power penalty is the modulation format difference before and after switching. Assuming the same modulation index, in order to get the same RF power achieving the same signal-to-noise ratio (SNR), more optical power is needed for the OSSB modulation format compared with the DSB modulation format.

The transmission performance of the OSSB switched signals in an optical link is investigated. The transmission responses over a 9-km single mode fiber (SMF) optical link with and without the photonic microwave switching based on wavelength down-conversion are shown in Fig. 7. Since the signal without the proposed switching has a DSB modulation format, it will undergo serious dispersion-induced RF power fading, especially at the points of 20.48 and 35.26 GHz. On the other hand, the transmission response of the optical link

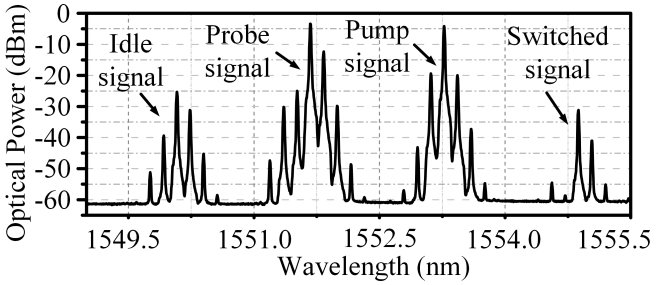

Fig. 8. Measured optical spectrum at the SOA's output for photonic microwave switching based on wavelength up-conversion.

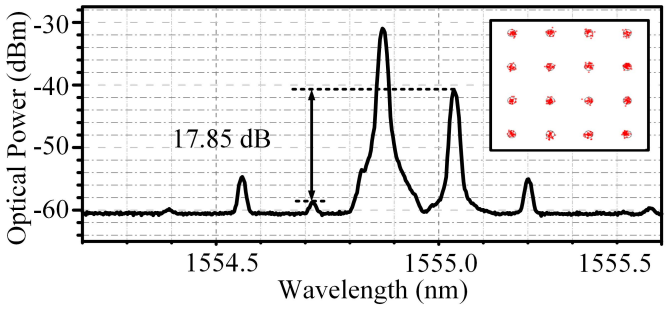

Fig. 9. Measured optical spectrum of the switched signal with the carrier wavelength of 1554.91 nm for photonic microwave switching based on wavelength up-conversion. Inset: measured constellation diagram with the optical power received by the PD being −2 dBm.

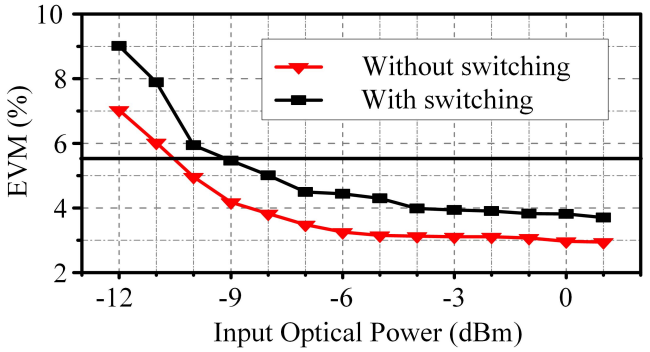

Fig. 10. Measured EVM values versus the optical power received by the PD without and with the photonic microwave switching based on wavelength up-conversion.

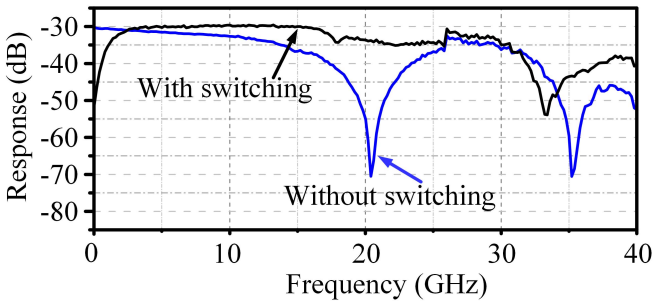

Fig. 11. Measured transmission responses over a 9-km optical link with and without the photonic microwave switching based on wavelength up-conversion.

with the proposed photonic microwave switching is relatively flat. For the frequencies higher than 35 GHz, the frequency response with the photonic microwave switching is going down, limited mainly by the SOA's carrier recovery time.

The photonic microwave switching based on OSSB wavelength up-conversion, by which the switched optical carrier's wavelength (ω_{cs}) is longer than the probe signal's wavelength (ω_{probe}), is also implemented. The probe and pump signals' wavelengths are set to be 1551.71 and 1553.31 nm, respectively. The optical power of the probe and the pump are 2.41 and 0.52 dBm, respectively, so the probe-pump power ratio is 1.89 dB.

Fig. 8 shows the optical spectrum at the SOA's output for photonic microwave switching based on wavelength up-conversion. The signal is copied to the wavelength of 1554.91 nm successfully, and the switched signal is an OSSB-modulated signal. Fig. 9 shows the switched signal's optical spectrum in detail. The SSR is 17.85 dB. The constellation diagram is also shown when the optical power received by the PD is −2 dBm, giving an EVM value of 3.805%.

Fig. 10 shows the EVM values versus the optical power received by the PD for the conditions with and without the photonic microwave switching based on wavelength up-conversion, respectively. The photonic microwave switching introduces a 1.39-dB power penalty if the EVM threshold of 5.6% is applied. This power penalty is smaller than that based on wavelength down-conversion. However, the EVM degradation at high input optical power regime is relatively large, as compared with Fig. 7. The transmission performance of the OSSB switched signal in the 9-km SMF link is shown in Fig. 11. By introducing the OSSB switching, the chromatic dispersion-induced RF power fading effect is effectively suppressed. By comparing Figs. 7 and 11, the frequency response in the wavelength up-conversion case is generally smaller than that of the wavelength down-conversion case, because the conversion efficiency based on FWM effect in SOA for wavelength down-conversion is larger than that for wavelength up-conversion [23], [24], [27].

B. Investigation of the Key Parameters Influences

The performance of the photonic microwave switching can be evaluated by the SSR and the EVM of the OSSB switched signal. Based on (2), the SSR value is affected by the modulation depth of the optical probe signal, the optical pump and probe power injected into the SOA, and the SOA's overall saturation level (partly related to the SOA's bias current). In order to optimize the system performance, the influences of the system's key parameters, i.e., the optical probe and pump power, the optical probe-to-pump power ratio, modulation depth and the bias current of the SOA, are investigated.

Fig. 12(a) shows the SSR versus the total injected optical power. The wavelengths of the probe and the pump are fixed at 1551.71 and 1550.14 nm, respectively, and the optical probe-pump power ratio is fixed at 0 dB. The RF signal's power is set to be 6 dBm. The SOA is biased with a current of 185 mA. As can be seen, with the total input optical power increased from around −3 dBm, the SSR value increases.

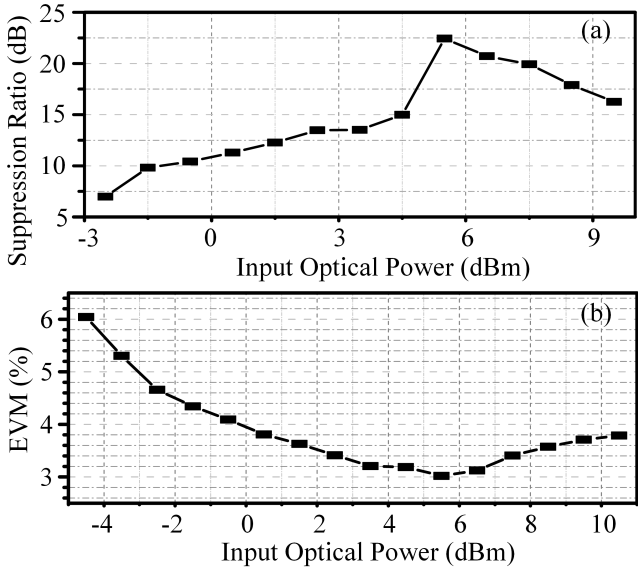

Fig. 12. (a) Measured SSR and (b) measured EVM of the switched signal with the wavelength of 1548.33 nm versus the total injected optical power.

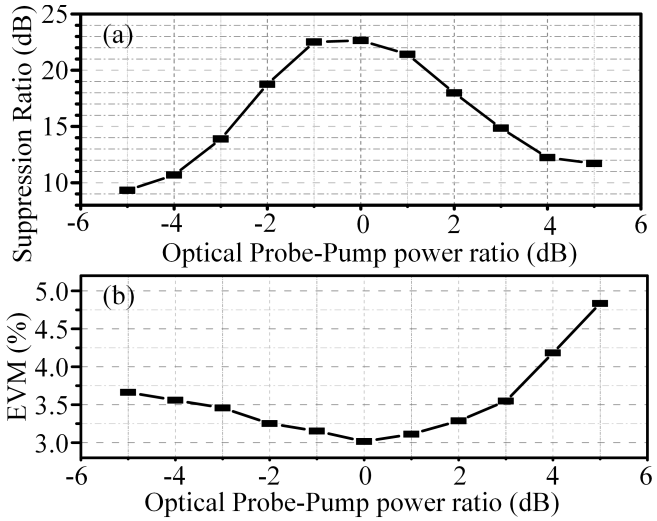

Fig. 13. (a) Measured SSR and (b) measured EVM of the switched signal at 1548.33 nm versus the optical probe-pump power ratio.

When the total injected power is tuned to be 5.46 dBm, the SSR reaches its maximal value of 22.65 dB. Then, the SSR value decreases with the increasing of the total injected optical power. Fig. 12(b) shows the EVM value versus the total injected optical power when a 200-Mb/s 16-QAM RF signal centered at 20 GHz is modulated. With the total injected optical power of 5.46 dBm, the minimal EVM of 3.019% is observed. An optimum value of the injected optical power exists, and low optical SNR causes the results left from the optimum point, while the SOA's deep gain saturation causes the results right from the optimum point.

Fixing the total input optical power at 5.46 dBm, the influence of the optical probe-pump power ratio on the performance of photonic microwave switching can be investigated. As shown in Fig. 13, there also exists an optimal optical probe-pump power ratio (about −0.11 dB) for both the SSR and

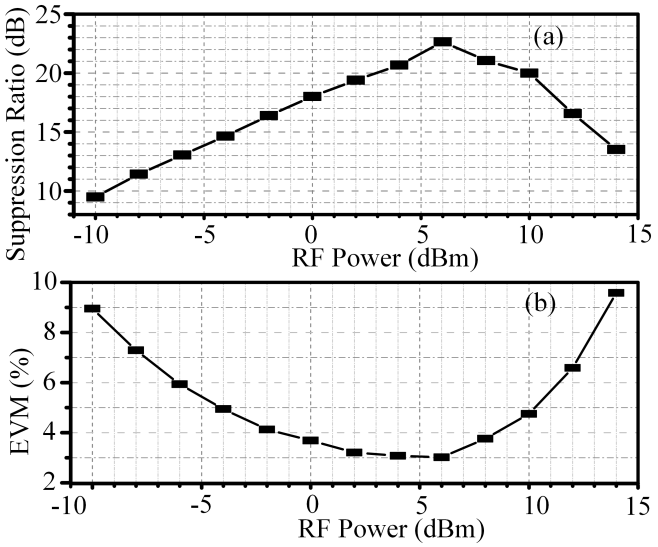

Fig. 14. (a) Measured SSR and (b) measured EVM of the switched signal at 1548.33 nm versus the 20-GHz RF signal's power.

the EVM performance of the switched signal. We ascribe this to FWM efficiency's dependence on the optical probe-pump power ratio in the SOA [24], [29]. From (2), the generation of signals at new wavelengths is contributed jointly by both the amplitudes of the optical probe and pump signals injected into the SOA. Thus, an optimum pump power exists for a probe power value when the total input optical power is fixed, which means that an optimum optical probe-pump power ratio exists.

Fig. 14 shows the impact of the modulated RF signal's power on the SSR and EVM of the switched signal. The SOA is biased at 185 mA. The power of the 1551.71-nm probe signal is 2.41 dBm, and that of the 1550.14-nm pump signal is 2.52 dBm. Fig. 14(a) shows the SSR of the switched signal versus the modulated 20-GHz RF signal's power. As can be seen, there exists an optimal RF power (i.e., 6 dBm) with which the SSR has the largest value of 22.65 dB. Fig. 14(b) shows the EVM of the switched signal versus the modulated RF signal's power. With the optimal RF power of 6 dBm, the EVM reaches its smallest value of 3.019%. When the RF power is lower than 6 dBm, the EVM value decreases with the RF power's increasing, because the modulation depth as well as the SNR is increased. When the RF power is higher than the optimal value, the increasing of the RF power leads to the increasing of the EVM value, which is due to the modulation nonlinearity of the MZM.

The influence of the SOA's bias current is also investigated. The results are shown in Fig. 15. Being modulated by a 20-GHz 6-dBm RF signal, the 1551.71-nm 2.41-dBm probe signal is combined with the 1550.14-nm 2.52-dBm pump signal and then injected into the SOA. As shown in Fig. 15(a), the optimal SOA bias current to achieve the best SSR performance is 185 mA. In addition, the best EVM of 3.019% is also achieved when the bias current of the SOA is 185 mA. This is because many of the parameters in (2), in general, depend on the overall saturation level of the SOA [24]. An optimum bias current of the SOA exists to achieve a proper overall saturation level and make the performance optimum.

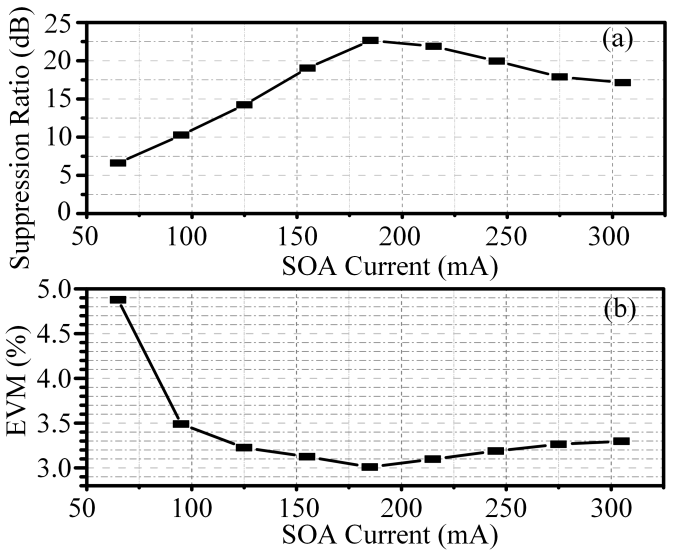

Fig. 15. (a) Measured SSR and (b) measured EVM values of the switched signal at 1548.33 nm versus the SOA bias currents.

The set of the optimized key parameters for the wavelength up-conversion condition can also be investigated in the same way. The relationship between the parameters and the system performance are the same for the case of wavelength down-conversion. When the wavelength of the probe signal is set to be 1551.71 nm, and the pump signal is fixed at 1553.31 nm, and the optimized optical power of the probe and the pump are 2.41 and 0.52 dBm, respectively. The optimized total input optical power is 2.93 dBm, and the optimized probe-pump power ratio is 1.89 dB. The SOA bias current is 185 mA. With these optimized parameter values, the SSR performance of the system is 17.85 dB, and the EVM value is 3.805% when the optical power injected into the PD is -2 dBm. It can be seen that the optimized parameters for the two cases have different values. This is mainly due to the difference of the conversion efficiency based on FWM effect in SOA between wavelength down- and up-conversion.

IV. Conclusion

A novel photonic microwave switching was proposed and investigated based on OSSB wavelength conversion in an SOA. The fast response of the SPM and FWM in the SOA guarantees fast switching speed, and the FWM makes the photonic microwave switch transparent for modulation format and data rate over a wide wavelength range. In addition, OSSB modulation occupies the least optical bandwidth, which minimizes the crosstalk of the system and overcomes the dispersion-induced RF power fading in long-distance RoF systems. The proposed scheme could have a wide wavelength range, and allow a large RF bandwidth especially in the high-frequency regime. A 200-Mb/s 16-QAM centered at 20 GHz is experimentally switched to a targeted path, and an OSSB modulation with an SSR of 22.65 or 17.85 dB is generated for the photonic microwave switching based on wavelength down- or up-conversion, respectively. The scheme is simple, since only a single SOA is used, which can find application in the future microwave photonic systems.

References

[1] X. Qian, P. Hartmann, S. Li, R. Penty, and I. H. White, "Application of semiconductor optical amplifiers in scalable switched radio-over-fiber networks," in *Proc. IEEE Int. Topical Meeting Microw. Photon.*, Oct. 2005, pp. 317–320.

[2] G. C. Tavik *et al.*, "The advanced multifunction RF concept," *IEEE Trans. Microw. Theory Techn.*, vol. 53, no. 3, pp. 1009–1020, Mar. 2005.

[3] S. Pan *et al.*, "Satellite payloads pay off," *IEEE Microw. Mag.*, vol. 16, no. 8, pp. 61–73, Sep. 2015.

[4] M. Sotom, B. Benazet, A. L. Kernec, and M. L. Maignan, "Microwave photonic technologies for flexible satellite telecom payloads," in *Proc. ECOC*, 2009, pp. 1–4.

[5] I.-S. Joe and O. Solgaard, "Scalable optical switch fabric for avionic networks," in *Proc. Avionics Fiber-Optics Photon.*, Sep. 2005, pp. 19–20.

[6] K. Xu *et al.*, "Microwave photonics: Radio-over-fiber links, systems, and applications," *Photon. Res.*, vol. 2, no. 4, pp. B54–B63, Aug. 2014.

[7] M. Crisp, E. T. Aw, A. Wonfor, R. V. Penty, and I. H. White, "Demonstration of an SOA efficient 32×32 optical switch for radio over fiber distribution systems," in *Proc. OFC*, Feb. 2008, pp. 1–3, paper OThP4.

[8] N. K. Dutta and Q. Wang, *Semiconductor Optical Amplifiers*. 2nd ed., Singapore: World Sci., 2013.

[9] T. Durhuus, B. Mikkelsen, C. Joergensen, S. L. Danielsen, and K. E. Stubkjaer, "All-optical wavelength conversion by semiconductor optical amplifiers," *J. Lightw. Technol.*, vol. 14, no. 6, pp. 942–954, Jun. 1996.

[10] S. Singh, X. Ye, and R. Kaler, "All optical wavelength conversion based on cross polarization modulation in semiconductor optical amplifier," *J. Lightw. Technol.*, vol. 31, no. 11, pp. 1783–1792, Jun. 2013.

[11] H. Yang, Y. Shi, C. M. Okonkwo, E. Tangdiongga, and A. M. J. Koonen, "Dynamic capacity allocation in radio-over-fiber links," in *Proc. IEEE Topical Meeting Microw. Photon.*, Oct. 2010, pp. 181–184.

[12] G. H. Smith, D. Novak, and Z. Ahmed, "Overcoming chromatic-dispersion effects in fiber-wireless systems incorporating external modulators," *IEEE Trans. Microw. Theory Techn.*, vol. 45, no. 8, pp. 1410–1415, Aug. 1997.

[13] S. R. Blais and J. Yao, "Optical single sideband modulation using an ultranarrow dual-transmission-band fiber Bragg grating," *IEEE Photon. Technol. Lett.*, vol. 18, no. 21, pp. 2230–2232, Nov. 1251, 2006.

[14] H. K. Sung, E. K. Lau, and M. C. Wu, "Optical single sideband modulation using strong optical injection-locked semiconductor lasers," *IEEE Photon. Technol. Lett.*, vol. 19, no. 13, pp. 1005–1007, Jul. 2007.

[15] Y. Shen, X. Zhang, and K. Chen, "Optical single sideband modulation of 11-GHz RoF system using stimulated Brillouin scattering," *IEEE Photon. Technol. Lett.*, vol. 17, no. 6, pp. 1277–1279, Jun. 2005.

[16] Y. M. Zhang, F. Z. Zhang, and S. L. Pan, "Optical single sideband polarization modulation for radio-over-fiber system and microwave photonic signal processing," *Photon. Res.*, vol. 2, no. 4, pp. B80–B85, Aug. 2014.

[17] M. Xue, S. L. Pan, and Y. J. Zhao, "Optical single-sideband modulation based on a dual-drive MZM and a 120° hybrid coupler," *J. Lightw. Technol.*, vol. 32, no. 19, pp. 3317–3323, Oct. 2014.

[18] U.-S. Lee, H.-D. Jung, and S.-K. Han, "Optical single sideband signal generation using phase modulation of semiconductor optical amplifier," *IEEE Photon. Technol. Lett.*, vol. 16, no. 5, pp. 1373–1375, May 2004.

[19] H. Jiang *et al.*, "Improved optical single-sideband generation using the self-modulation birefringence difference in semiconductor optical amplifiers," *Opt. Lett.*, vol. 32, no. 17, pp. 2580–2582, Sep. 2007.

[20] M. Park and J.-I. Song, "All-optical frequency upconversion of a quasi optical single sideband signal utilizing a nonlinear semiconductor optical amplifier for radio-over-fiber applications," *Opt. Exp.*, vol. 19, no. 24, pp. 24499–24506, Nov. 2011.

[21] P. H. Hsie, W. S. Tsai, C. C. Weng, and H. H. Lu, "Optical single sideband modulation of 9-GHz RoF system based on FWM effects of SOA," in *Proc. PIERS*, 2011, pp. 918–921.

[22] D. Zhu, H. Wu, and S. L. Pan, "Photonic switching of RF signals based on optical single sideband wavelength conversion in a semiconductor optical amplifier," in *Proc. ICOCN*, Nov. 2014, pp. 1–3, paper M43.

[23] M. Felicetti, J. J. Van der Tol, E. J. Geluk, D. Pustakhod, M. J. Wale, and M. K. Smit, "Integrated high-performance TE/TM converters for polarization independence in semiconductor optical amplifiers," *J. Lightw. Technol.*, vol. 33, no. 17, pp. 3584–3590, Sep. 2015.

[24] D. F. Geraghty, R. B. Lee, M. Verdiell, M. Ziari, A. Mathur, and K. J. Vahala, "Wavelength conversion for WDM communication systems using four-wave mixing in semiconductor optical amplifiers," *IEEE J. Sel. Topics Quantum Electron.*, vol. 3, no. 5, pp. 1146–1155, Oct. 1997.

[25] K. Kikuchi, M. Kakui, C.-E. Zah, and T.-P. Lee, "Observation of highly nondegenerate four-wave mixing in 1.5 μ traveling-wave semiconductor optical amplifiers and estimation of nonlinear gain coefficient," *IEEE J. Quantum Electron.*, vol. 28, no. 1, pp. 151–156, Jan. 1992.

[26] S. Bandyopadhyay, Y. Hong, P. S. Spencer, and K. A. Shore, "Simple techniques for highly efficient wavelength conversion with low polarization sensitivity by use of semiconductor optical amplifiers," *J. Opt. Soc. Amer. B, Opt. Phys.*, vol. 21, no. 5, pp. 1023–1031, 2004.

[27] A. D'Ottavi, P. Spano, G. Hunziker, R. Paiella, R. Dall'Ara, G. Guekos, and K. J. Vahala, "Wavelength conversion at 10 Gb/s by four-wave mixing over a 30-nm interval," *IEEE Photon. Technol. Lett.*, vol. 10, no. 7, pp. 952–954, Jul. 1998.

[28] D. Zhu, S. F. Liu, and S. L. Pan, "Multichannel up-conversion based on polarization-modulated optoelectronic oscillator," *IEEE Photon. Technol. Lett.*, vol. 26, no. 6, pp. 544–547, Mar. 2014.

[29] A. D'Ottavi *et al.*, "Four-wave mixing in semiconductor optical amplifiers: A practical tool for wavelength conversion," *IEEE J. Sel. Topics Quantum Electron.*, vol. 3, no. 2, pp. 522–528, Apr. 1997.

Dan Zhu (M'12) received the B.S. and Ph.D. degrees in electronics engineering from Tsinghua University, Beijing, China, in 2004 and 2009, respectively.

In 2009, she joined the Research Department of Radar Signal Processing, the 14th Research Institute, China Electronics Technology Group Corporation, as a Researcher. In 2011, she joined the Key Laboratory of Radar Imaging and Microwave Photonics, Ministry of Education, Nanjing University of Aeronautics and Astronautics, Nanjing, China, where she is currently an Associate Professor. Her current research interests include photonic microwave and millimeter wave generation and optical signal processing.

Dr. Zhu is a member of the IEEE Microwave Theory and Techniques Society, the IEEE Photonics Society, and the Optical Society of America.

Zhengwu Wei, photograph and biography not available at the time of publication.

Huan Wu, photograph and biography not available at the time of publication.

Shilong Pan (S'06–M'09–SM'13) received the B.S. and Ph.D. degrees in electronics engineering from Tsinghua University, Beijing, China, in 2004 and 2008, respectively.

From 2008 to 2010, he was a Vision 2010 Post-Doctoral Research Fellow with the Microwave Photonics Research Laboratory, University of Ottawa, Ottawa, ON, Canada. He joined the College of Electronic and Information Engineering, Nanjing University of Aeronautics and Astronautics, China, in 2010, where he is currently a Full Professor and the Executive Director of the Key Laboratory of Radar Imaging and Microwave Photonics, Ministry of Education. He has authored or co-authored over 260 research papers, including over 140 papers in peer-reviewed journals and 120 papers in conference proceedings. His current research interests include microwave photonics, which includes optical generation and processing of microwave signals, analog photonic links, photonic microwave measurement, and integrated microwave photonics.

Dr. Pan is a Senior Member of the IEEE Microwave Theory and Techniques Society, the IEEE Photonics Society, and the IEEE Instrumentation and Measurement Society. He is a member of the Optical Society of America. He was selected to receive an OSA Outstanding Reviewer Award in 2015. He serves as the Chair of numerous international conferences and workshops, including the TPC Chair of the International Conference on Optical Communications and Networks in 2015, the TPC Chair of the High-Speed and Broadband Wireless Technologies Subcommittee of the IEEE Radio Wireless Symposium in 2013, 2014, and 2016, the TPC Chair of the Optical Fiber Sensors and Microwave Photonics Subcommittee of the OptoElectronics and Communication Conference in 2015, and the Chair of the Microwave Photonics for Broadband Measurement Workshop of the International Microwave Symposium in 2015.